Colloid Polym Sci (2007) 285:515–521
DOI 10.1007/s00396-006-1592-6

ORIGINAL CONTRIBUTION

Thermosensitive phase behavior and drug release of in situ gelable poly(*N*-isopropylacrylamide-co-acrylamide) microgels

Qin Wang · Yanbing Zhao · Yajiang Yang · Huibi Xu · Xiangliang Yang

Received: 11 July 2006 / Accepted: 27 September 2006 / Published online: 21 November 2006

Abstract In situ gelable poly(*N*-isopropylacrylamide-co-acrylamide) microgels were prepared by precipitation polymerization in the presence of various amounts of *N*, *N*′-methlenebisacrylamide as a crosslinker. The diameters of microgels were in the range of 200–300 nm with narrow distributions as determined by photo correlation spectroscopy. The equilibrium swelling ratio and thermosensitive properties of the microgels increased with decreasing crosslinker content. The volume phase transition of microgels dispersions at high concentrations were investigated by phase diagrams. The microgels dispersions experienced four phases when the temperature was increased: semitranslucent swollen gel, clear flowable suspension, cloud flowable suspension, and white shrunken gel. The related phase transition temperatures were influenced by crosslinker content and the concentration of the microgel dispersions. Herein, the gelation temperature was changed by more than 20 °C, shrinking temperatures were slightly changed by about 3 °C, and cloud point temperatures showed almost no change. The three phase transition temperatures of microgels dispersed in phosphate-buffered saline solutions were lower than that in water. As drug carriers, the release rates of bleomycin from bleomycin-loaded microgel dispersions exhibited diffusion control at human body temperature.

Q. Wang · Y. Zhao · Y. Yang (✉) · H. Xu
Department of Chemistry,
Huazhong University of Science and Technology,
Wuhan 430074, China
e-mail: yjyang@mail.hust.edu.cn

X. Yang
College of Life Science and Technology,
Huazhong University of Science and Technology,
Wuhan 430074, China

Keywords In situ gelable · Microgel · Thermosensitive phase transition · Drug release

Introduction

Injectable liquids can form semisolid gels after being introduced into the body through a catheter, i.e., *undergoing* in situ gel forming, which could be used in the fields of parenteral drug delivery systems, embolization, tissue engineering, etc. [1–3]. The advantages of in situ gel forming include small wounds and the ease of administering them as implants. As drug delivery carriers, they enhance bioavailability and reduce the side effects of drugs. There are several methods for achieving in situ gel forming, such as in situ photopolymerization [4], precipitation by solvent changes [5], ionic cross-linking [6], pH [7] or temperature-induced gelling [1], and other methods [8].

In the past few decades, much attention has been paid to temperature-induced gelling systems because temperature is the only modulation factor for gel forming [1, 9] for systems like polysaccharides [10], polymers based on *N*-isopropylacrylamide (NIPAAm) [11, 12], tri-block copolymers consisting of hydrophilic and hydrophobic chains such as poloxamer [13, 14], poly(ethylene oxide) (PEO)-poly(L-lactic acid)-PEO copolymers [15], etc. These gelling systems show lower critical solution temperatures (LCST). For example, the LCST of NIPAAm homopolymer in water is about 32 °C, near the temperature of the human body [16], and can be easily manipulated by copolymerizing with other hydrophilic or hydrophobic comonomers [17]. Aqueous poly(*N*-isopropylacrylamide-co-acrylic acid) solutions [18] and interpenetrating polymer networks nanoparticles consisting of poly(NIPAAm) and polyacrylic acid [19] were developed as inverse thermoreversible

gelation systems which are flowable at room temperature and become gel over LCST.

Microgel dispersion behaves differently from the above polymer solutions. It is a crosslinked gel dispersed in aqueous media. The average diameters of microgels are usually in the range of 50 nm–5 μm [20]. Temperature-sensitive microgels possess temperature-dependent swelling or shrinking behavior and undergo a significant volume change at a certain temperature, the so-called volume phase transition temperature [20]. In contrast with solutions of linear polymers, the advantages of microgel dispersion are low viscosity at high solid contents, very high surface areas, and rapid thermal response [21]. They are widely applied in the fields of biotechnology [22, 23] as drug delivery systems [24, 25], as reactors for inorganic nanoparticles [26], and as matrices for polymerization [27]. The phase behavior of the diluted poly (NIPAAm) microgel dispersions has been discussed elsewhere [28, 29]. Richtering and coworkers compared the phase behaviors and rheological properties of poly (NIPAAm) microgel dispersions to linear poly(NIPAAm) solutions at various concentrations, especially focusing on structure formation [30]. The rheological behaviors of concentrated poly(NIPAAm) microgel dispersions depend more strongly on the temperature than that of linear poly (NIPAAm) [31].

In the present work, a series of temperature-sensitive poly(*N*-isopropylacrylamide-co-acrylamide) [Poly (NIPAAm-co-AAm)] microgels were prepared in the presence of various contents of crosslinker. The temperature-sensitive properties, phase transitions, and drug release profiles of the microgel dispersions at high concentrations were studied in this work.

Materials and methods

Materials

NIPAAm (Acros) and *N*,*N*′-methylenebisacrylamide (MBAAm, Tianjin Kermel) were recrystallized from n-hexane and methanol, respectively. Bleomycin (BLM) A5 hydrochloride employed for injection was purchased from Tianjin Taihe. Other reagents were of analytic grade and used as received. Milli-Q ultra-pure water was used through all experiments.

Preparation of poly(NIPAAm-co-AAm) microgels

Poly(NIPAAm-co-AAm) microgels were prepared using the precipitation polymerization described elsewhere [32]. NIPAAm (4.76 g), acrylamide (AAm, 0.53 g), varying amounts of MBAAm (0.04–0.06 g), and sodium dodecyl sulfate (0.08 g) were dissolved in 400 ml water in a flask equipped with a condenser and a gas inlet under stirring. After the solution was purged with nitrogen for about 30 min, potassium persulfate (0.22 g) was added as initiator into the mixture. Polymerization was carried out at 70 °C for 4 h. The resultant poly(NIPAAm-co-AAm) microgel dispersions were further dialyzed against water for 2 weeks to remove unreacted monomers and other impurities. A small quantity of dialyzed dispersion was taken for size analysis. The microgel dispersions were subsequently lyophilized to collect xerogel. The yields were about 90%. During the preparation of the microgels, the molar ratio of MBAAm as a crosslinker to all monomers was 0.5, 1, 2, 2.5, 5, and 7.3%, respectively (the samples were designated as microgel 1–6).

Photo correlation spectroscopy

The hydrodynamic diameters of microgel particles were measured at various temperatures ranging from 25 to 50 °C by dynamic light scattering (Nano-ZS 90, Malvern) equipped with a He–Ne laser (λ=633 nm). All samples were diluted with water and maintained at the designed temperature for 3 min before testing. The swelling ratio (SR) of the microgel was defined as follows [33]:

$$SR = V_{\mathrm{swol}}/V_{\mathrm{shru}} = (D_{\mathrm{swol}}/D_{\mathrm{shru}})^3 = (D_{25}/D_{50})^3 \qquad (1)$$

where V_{swol} and V_{shru} are swollen and shrunken volumes of microgel particles. D_{25} and D_{50} are the average diameters of the microgel particles at 25 and 50 °C, respectively.

Phase diagram of the microgel dispersions

Microgel dispersions with various concentrations were obtained when 1 ml of water or phosphate-buffered saline (PBS, pH 7.4, ionic strength 0.2 mol/l) solution were added into a 5-ml test tube containing 0.05–0.25 g of freeze-dried microgel powder. The microgel dispersions were kept overnight at room temperature. The phase transition temperature of microgel dispersions was determined in a water bath by vial inverting combined with visual method [34] in the range of 5–50 °C.

Rheological measurements

The storage modulus (G′) and the loss modulus (G″) of microgel dispersions were determined using a strain-controlled rheometer (ARES 2000, TA) equipped with a parallel plate (Φ25 mm) and the gap set at 0.9 mm in the temperature range of 15–50 °C. The strain was 3%. The heating rate was 3 °C/min. The frequency was 1.0 rad/s.

In vitro release studies

BLM, a water-soluble cytotoxic drug currently used in anticancer chemotherapy, was used as a model drug in this study. The drug-loading and in vitro release experiments were preformed in a method similar to that described elsewhere [35]. Briefly, the xerogel powder was swollen completely in a saline or PBS solution at a suitable temperature to form a flowable dispersion. Then, BLM was added to the microgel dispersion at a concentration of 1.0 mg/ml. The mixture was then either vortexed or tumbled to form a uniform suspension. The drug-loaded microgel dispersion (1.0 ml) was poured into a colorimetric tube placed in a 37 °C water bath. The drug-loaded microgel dispersion immediately became a semisolid gel and was subsequently incubated for 10 min. The release medium (10 ml) was added into the colorimetric tube. The mixed solution (1 ml) was removed from the tube at designed time intervals for testing of drug release. Simultaneously, fresh release solutions of 1 ml were replenished into the colorimetric tube. The amount of released drug was determined by absorbance measurements at a wavelength of 295 nm using a UV spectrophotometer (UV-2102 PC, UNICO). All experiments were performed in triplicate.

Results and discussion

Characterization of poly(NIPAAm-co-AAm) microgels

The average hydrodynamic diameter, polydispersity index (PDI) of size distribution at 25 °C and swelling ratio (SR) of the microgel particles are listed in Table 1. The sizes of the microgel particles are in the range of 200–300 nm and the PDIs are about 0.08 near monodispersion.

Figure 1 shows the equilibrium hydrodynamic diameters of microgel particles at various temperatures. The diameters of the microgel particles, prepared using various crosslinker contents, decreased with increasing temperature. When the crosslinker contents are lower than 5 mol%, the diameters of the microgel particles exhibit an abrupt change in the range of 35–40 °C. In the case of crosslinker contents of more than 5 mol%, the abrupt changes are not found. This is in accordance with previous results [21]. Therefore, the microgels with lower crosslinking densities exhibit a more flexible network and are more sensitive to temperature variation [36]. The swelling ratios of the microgels calculated from the data in Fig. 1 are listed in Table 1.

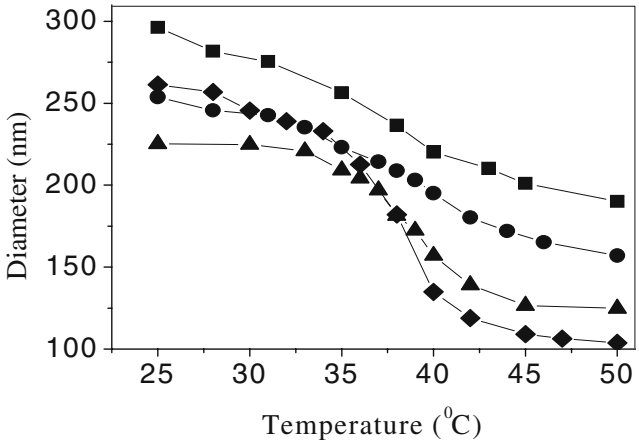

Fig. 1 Influence of temperature on the diameters of microgels particles. microgel 1 (*diamonds*), microgel 4 (*triangles*), microgel 5 (*circles*), microgel 6 (*squares*). The concentration of the microgel dispersions is 8×10^{-5} g/ml

Thermoreversible phase transition behavior

A typical volume phase transition behavior of the microgel dispersions at high concentrations is shown in Fig. 2. The microgel 4 dispersion (9 wt.% in PBS) exhibited four phases. Phase A (T<22 °C) is a semitranslucent swollen gel with blue emulsion light possibly owing to the increase of volume fraction of expanded microgel [37] at low temperatures. Richtering and Senff believed that colloidal crystals were formed by the closely packed soft microgel particles at high concentration and low temperature [38]. This semitranslucent swollen gel became a clear, flowable suspension (phase B) when the temperature was increased from 22 to 36 °C. Apparently, its fluidity is due to a collapsed particle size and weakened water–polymer hydrogen bonding upon an increasing of the temperature. Usually, the temperature-induced transition from a flowable suspension to a swollen gel is called the gelling temperature (GT). With a further increase of the temperature (36 °C< T<40 °C), hydrogen bonding of intra- and interpolymer chains and hydrophobic interactions between side-chains in poly(NIPAAm) take place and water becomes a rather poor

Table 1 Diameters, distribution at 25 °C and swelling ratio of the microgel particles

Parameters	Microgel 1	Microgel 2	Microgel 3	Microgel 4	Microgel 5	Microgel 6
Diameter (nm)	261.4	265.1	245.4	225.3	253.8	296.3
PDI	0.081	0.054	0.040	0.046	0.062	0.051
Swelling ratio (*SR*)	15.99	14.88	10.35	5.91	4.22	3.79

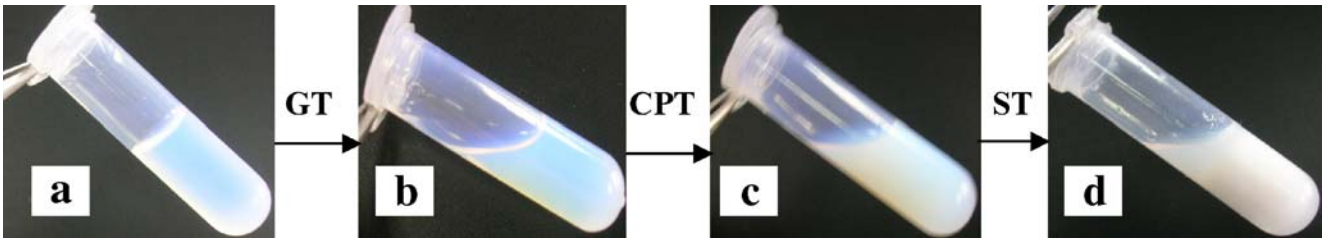

Fig. 2 Photographs of microgel 4 dispersion (9 wt.% in PBS). **a** semitranslucent swollen gel phase (T<22 °C); **b** clear suspension phase (22 °C< T<36 °C); **c** cloud suspension phase (36 °C< T<40 °C), and **d** white shrunken gel (T>40 °C)

solvent. The clear microgel suspension becomes cloudy (phase C). The related temperature of this phase transition is defined as the cloud point temperature (CPT). When the temperature is higher than the gel shrinking temperature (ST) (ca. 40 °C), the cloud suspension becomes a white, semisolid shrunken gel (phase D), which can be ascribed to the strong hydrophobic interaction potential between the particles. Meanwhile, water is expelled from the microgel network and the microgel further collapses to form aggregates of microgel particles. The higher the temperature is, the more water is expelled and the more pronounced the phase separation is.

Based on the four phases of the microgel dispersions at the various temperatures, the phase diagrams of microgel 4 dispersion in PBS solution (a) and the microgel 6 dispersion in water (b) (Fig. 3) were measured by combining visual inspection and a vial-inverting method [34]. Four phase areas of microgel 4 are clearly observed in Fig. 3. However, phase B (clear suspension) is not observed for the microgel 6 dispersion. This may be attributed to the low swelling ratio and high crosslinking density resulting in its GT being higher than the CPT. When the temperature reaches its CPT, the semitranslucent swollen gel directly becomes opaque.

In addition, the GT of microgel dispersions significantly increases by ca. 20 °C with an increase of the microgel concentration. Because the microgel is a temperature-sensitive system, fully swollen microgels (phase A) at low concentrations can only be formed at lower temperatures. In contrast to the high temperatures, the formation of phase A needs a higher concentration because of the small size of the microgel particles. On the other hand, the ST decreases slightly with an increase of the microgel concentration. A possible explanation is that the enhanced hydrophobic interaction between the polymer's side-chains at high concentrations may result in the occurrence of a phase separation. However, the CPT is almost independent of the microgel concentration. This is in accordance with the situation for normal poly(NIPAAm) microgel [31]. As shown in Fig. 3, the three phase transition temperatures can close to a point. This appears to indicate that a swollen gel could turn into a shrunken gel directly upon a further increase of the concentration. Nevertheless, the maximum concentration of microgel is restricted by the swelling ratio of the microgel required for a uniform dispersion. On the other hand, there is a minimum gelling concentration for microgel dispersions similar to other thermal reduced gelation solutions [18].

The effects of crosslinker content on the volume phase transition behavior of microgel dispersions is shown in Fig. 4. It suggests that the GT is increased about 20 °C, the ST is increased by about 3 °C, while the CPT almost remains constant with an increase of crosslinker content in the tested range. Particularly, the GT is increased dramatically when the crosslinker content is lower than 2 mol%.

In order to further investigate the volume phase transitions of the concentrated microgel dispersions, the phase diagrams of the microgel 5 dispersed both in water and in PBS solution were determined (Fig. 5). It is found that the three phase transition temperatures in PBS solution are lower than that in water. This is in accordance with the

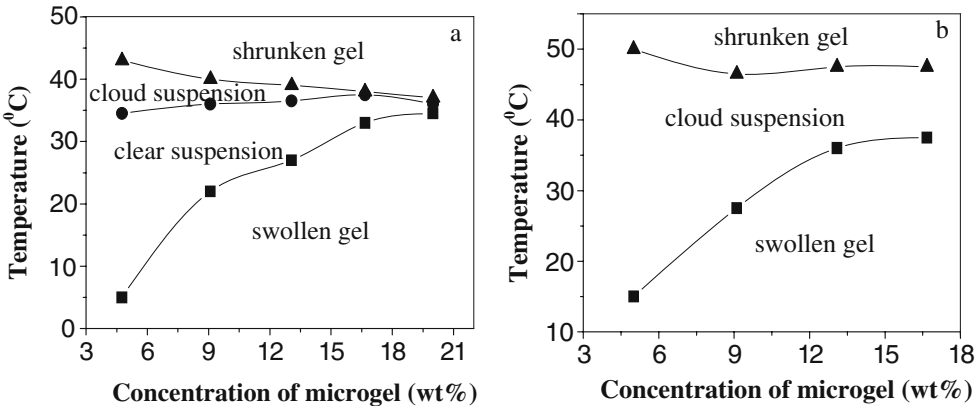

Fig. 3 Phase diagrams of a microgel 4 dispersion in PBS solution (**a**) and microgel 6 dispersion in water (**b**). GT (*squares*), CPT (*circles*), ST (*triangles*)

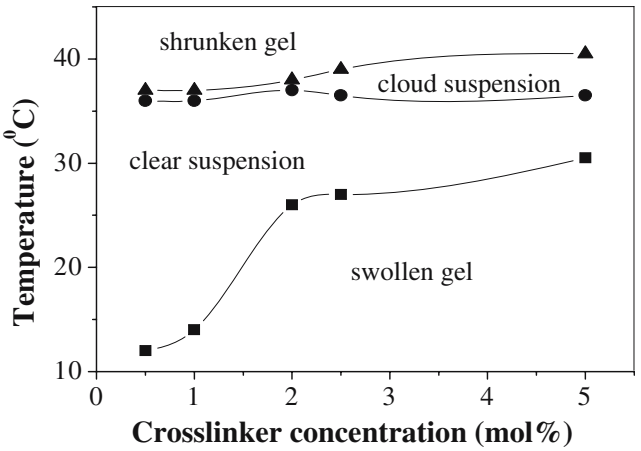

Fig. 4 Effect of the crosslinker content on the volume phase transition of microgel dispersions in PBS solution at a microgel concentration of 13 wt.%. GT (*squares*), CPT (*circles*), ST (*triangles*)

effect of salt on the LCST of poly(NIPAAm) [39]. A possible explanation is that the interaction between the microgel and water is weakened by the phosphate groups present in PBS solution [40].

Figure 6 shows the module of a microgel 4 dispersion (9 wt.%) in PBS solution as a function of temperature. Both the storage module (G′) and the loss module (G″) experience four steps upon an increase of the temperature. First, the swollen gel with high modules turns into a clear, flowing suspension with low modules and then becomes a cloudy suspension at CPT. Finally, the modules of the system increase rapidly till a shrunken gel is formed with a maximum module at ST. This experiment further confirms the occurrence of four phases of the microgel dispersions as described above. Furthermore, all values of G′ are higher than those of G″ in the tested temperature range, as shown in Fig. 6, indicating that an elastic behavior is predominant [41].

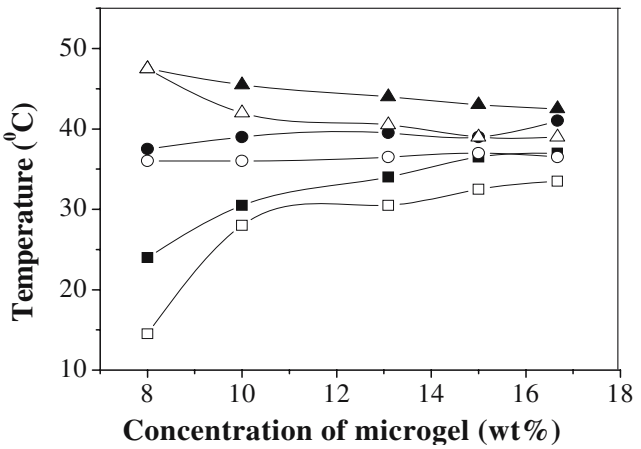

Fig. 5 Effect of dispersion media on the phase transition of microgel 5. GT (*solid* and *hollow squares*), CPT (*solid* and *hollow circles*), ST (*solid* and *hollow triangles*). *Solid symbols* are used for water and *hollow symbols* for PBS solution

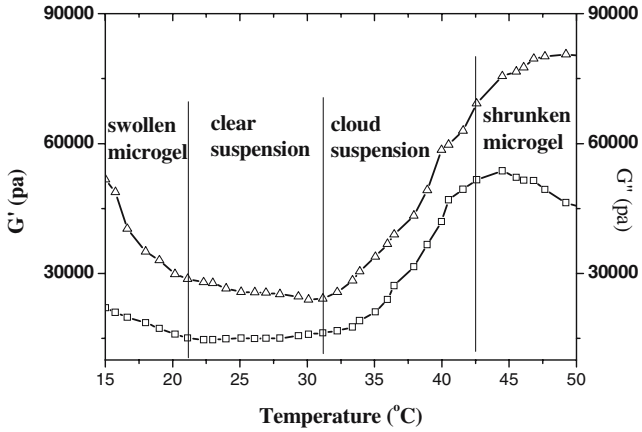

Fig. 6 Plot of storage modulus (G′) and loss modulus (G″) of microgel 4 dispersion (9 wt.%) in PBS solution vs temperature. G′ (*triangles*), G″ (*squares*)

Drug release

As an in situ gelable material used as drug carrier, for example as embolus or implant, a suitable transition temperature from flowing to nonflowing and a broader temperature range for the flowing phase are necessary. As described in Fig. 3b, the GT of the microgel 6 dispersion (17 wt.% in water) is approximately 37 °C, which is the human body temperature, whereas the ST is approximately 47 °C. The temperature range for the flowing phase is about 10 °C. In other words, the microgel 6 dispersion could be prepared at a temperature higher than 37 °C and still maintain its fluidity. After entering the body by injection, the microgel dispersion becomes a swollen gel at body temperature. Contrastingly, microgel 2 dispersion (13 wt.% in PBS solution) is flowable at room temperature and becomes a white, shrunken gel without fluidity at 37 °C, as shown in Fig. 3a. Its advantage is in its being flowable at lower temperatures and gelable at higher temperatures, which is more convenient for in situ gel forming.

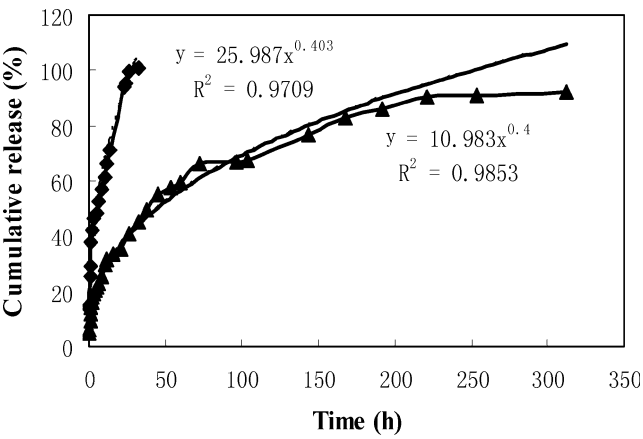

Fig. 7 In vitro cumulative percent release of BLM A5 Hydrochloride from microgel. *Diamonds* are used for microgel 2, *triangles* for microgel 6

Based on the above considerations, microgel 2 dispersions and microgel 6 dispersions can be employed as in situ gelable drug carriers and BLM can be used as a model drug in the present study. Figure 7 shows the BLM release profiles from the microgels. The power law of Peppas empirical equation [42, 43], which is well-known for estimating drug release from polymeric systems, was used to fit the data of the rates of drug release. The obtained equations are:

$$w_1 = 25.987t^{0.403} \text{ for microgel 2, with a correlation coefficient } (r) \text{ of } 0.9853$$

$$w_2 = 10.983t^{0.400} \text{ for microgel 6, with a correlation coefficient } (r) \text{ of } 0.9926$$

Herein, w is the cumulative percent of release and t is the release time (in hours). Both power exponents (n) are 0.403 and 0.400. For a drug carrier with a cylindrical shape, a power exponent of less than 0.45 indicates that the drug release is governed by Fickian diffusion [42, 43]. Figure 7 also indicates that the drug release from the swollen gel of microgel 6 can sustain for ca. 10 days. It suggests a typical sustained release of the drug. By contrast, the drug release from the shrunken gel of microgel 2 maintains only for ca. 28 h. The cumulative percent of drug release within 5 h reaches 50%. This suggests a typical burst release due to the shrinking action of microgel 2 at the ST expelling water together with drug. It is important to note that both the swollen gel and the shrunken gel keep their gel status in the period of the release experiment. It would be beneficial to use them as embolic materials.

Conclusion

The temperature-sensitivity of poly(NIPAAm-co-AAm) microgels becomes weak with an increase of the crosslinker content. Microgel dispersions at high concentrations experience four phases with increasing temperature: a semi-translucent swollen gel, a clear suspension, a cloudy suspension, and a white shrunken gel. The phase diagrams of the microgel dispersions indicate that the GT increases remarkably with increasing crosslinker content and concentration of the microgel. The ST increases slightly with increasing crosslinker content, but decreases with increasing microgel concentration. The CPT almost remains constant at various crosslinker contents and microgel concentrations. Two types of microgel dispersions were used as BLM carriers based upon an analysis of the phase diagrams. One is flowable at elevated temperature and the other is flowable at room temperature. The gelation for both systems is carried out at body temperature. The release from the swollen gel is typically a sustained release controlled by Fickian diffusion.

Acknowledgement This work was financially supported by Natural Science Foundation of China (no. 29974012).

References

1. Ruel-Gariépy E, Leroux JC (2004) Eur J Pharm Biopharm 58: 409–426
2. Packhaeuser CB, Schnieders J, Oster CG, Kissel T (2004) Eur J Pharm Biopharm 58:445–455
3. Lia XW, Liu WG, Ye GX, Zhang BQ, Zhu DW, Yao KD, Liu ZQ, Sheng XZ (2005) Biomaterials 26:7002–7011
4. He L, Zhang SF, Jin SZ, Qi ZN (1995) Polym Int 38:211–214
5. Eliaz RE, Kost J (2000) J Biomed Mater Res 50:388–396
6. Van Tomme SR, van Steenbergen MJ, De Smedt SC, van Nostrum CF, Hennink WE (2005) Biomaterials 26:2129–2135
7. Srividya B, Cardoza RM, Amin PD (2001) J Control Release 73:205–211
8. Balakrishnan B, Jayakrishnan A (2005) Biomaterials 26:3941–3951
9. Jeong B, Kim SW, Bae YH (2002) Adv Drug Deliv Rev 54:37–51 (and references therein)
10. Chenite A, Chaput C, Wang D, Combes C, Buschmann MD, Hoemann CD, Leroux JC, Atkinson BL, Binette F, Selmani A (2000) Biomaterials 21:2155–2161
11. Lin HH, Cheng YL (2001) Macromolecules 34:3710–3715
12. Stile RA, Burghardt WR, Healy KE (1999) Macromolecules 32:7370–7379
13. Cohn D, Sosnik A, Levy A (2003) Biomaterials 24:3707–3714
14. Cabana A, Aït-Kadi A, Juhász J (1997) J Colloid Interface Sci 190:307–312
15. Jeong B, Bae YH, Lee DS, Kim SW (1997) Nature 388:860–862
16. Schild HG (1992) Prog Polym Sci 17:163–249
17. Yoshida R, Sakai Y, Okano T, Sakai K (1994) J Biomater Sci Polym Ed 6:585–598
18. Han CK, Bae YH (1998) Polymer 39:2809–2814
19. Xia XH, Hu ZB, Marquez M (2005) J Control Release 103:21–30
20. Pelton RH (2000) Adv Colloid Interface Sci 85:1–33
21. Senff H, Richtering W (2000) Colloid Polym Sci 278:830–840
22. Zhou G, Veron L, Elaissari A, Delair T, Pichot C (2004) Polym Int 53:603–608
23. Pichot C, Taniguchi T, Delair T, Elaïssari A (2003) J Dispers Sci Technol 24:423–437
24. Lopez VC, Hadgraft J, Snowden MJ (2005) Int J Pharm 292:137–147
25. Lin SY, Chen KS, Liang RC (2001) Biomaterials 22:2999–3004
26. Zhang JG, Xu SQ, Kumacheva E (2004) J Am Chem Soc 126:7908–7914
27. Mrkic J, Saunders BR (2000) J Colloid Interface Sci 222:75–82
28. Arleth L, Xia XH, Hjelm RP, Wu JZ, Hu ZB (2005) J Polym Sci B Polym Phys 43:849–860
29. Yin W, Yang H, Zhang XQ, Wang ZL, Ding YW, Zhang GZ, Cheng RS (2005) J Appl Polym Sci 96:583–588
30. Stieger M, Pedersen JS, Lindner P, Richtering W (2004) Langmuir 20:7283–7292
31. Stieger M, Richtering W (2003) Macromolecules 36:8811–8818

32. Pelton RH, Chibante P (1986) Colloids Surf 20:247–256
33. Crowther HM, Vincent B (1998) Colloid Polym Sci 276:46–51
34. Jeong B, Bae YH, Kim SW (1999) Macromolecules 32:7064–7069
35. Pechenov S, Shenoy B, Yang MX, Basu SK, Margolin AL (2004) J Control Release 96:149–158
36. Wolfe MS, Scopazzi CJ (1989) J Colloid Interface Sci 133:265–277
37. Hooper HH, Yu J, Sassi AP, Soane DS (1997) J Appl Polym Sci 63:1369–1372
38. Senff H, Richtering W (1999) J Chem Phys 111:1705–1711
39. Routh AF, Vincent B (2004) J Colloid Interface Sci 273:435–441
40. Eeckman F, Amighi K, Mos AJ (2001) Int J Pharm 222:259–270
41. Berlinova IV, Dimitrov IV, Vladimirov NG, Samichkov V, Ivanov Y (2001) Polymer 42:5963–5971
42. Ritger PL, Peppas NA (1987) J Control Release 5:23–26
43. Ritger PL, Peppas NA (1987) J Control Release 5:37–42